

Quenching of Hadron Spectra in a chemically equilibrating Quark-Gluon Plasma

B. K. Patra¹ and Madhukar Mishra²

¹ Dept. of Physics, Indian Institute of Technology Roorkee, Roorkee 247 667, India

² Dept. of Physics, Banaras Hindu University, Varanasi 221 005, India

Abstract

Using the Fokker-Planck equation we have studied the drag co-efficient $A(t)$ and the consequent shift $\Delta p_{\perp}(L)$ in the transverse momentum due to collisional energy loss of energetic partons while passing through a chemically equilibrating quark-gluon plasma. Based on these we estimate the quenching factor $Q(p_{\perp})$ when the medium is undergoing longitudinal expansion governed by master rate equations. In contrast to the case of chemically equilibrated plasma investigated earlier by Mustafa and Thoma [2] we find less quenching because our calculated $Q(p_{\perp})$ is always greater at all momenta. This result is attributed to the weak drag coefficient operating during initial state interactions.

PACS: 12.38.Bx; 24.85.+p

1 Introduction

The inclusive yield of hadrons produced with high transverse momentum p_\perp in Au+Au collisions at the Relativistic Heavy Ion Collider (RHIC) has recently been shown to be significantly suppressed in comparison with the cumulative yield of binary NN interactions. This effect, called “jet quenching”, is considered an important signal for the production of a quark-gluon plasma (QGP) and a vast literature [1]-[21] already exists dealing with the phenomenological/theoretical aspects of the said effect; see Appendix for a brief review.

Jet quenching is believed to occur due to the fact that hard partons produced at the initial stage of the heavy ion collision lose energy as they propagate through the fireball making $Q(p_\perp) < 1$. Here the quenching factor is experimentally defined by the ratio

$$Q(p_\perp) = \frac{\Sigma^{\text{med}}(p_\perp)}{\Sigma^{\text{vac}}(p_\perp)}; \quad \Sigma(p_\perp) = \frac{d^2\sigma(p_\perp)}{d^2p_\perp} \quad (1)$$

where $\Sigma(p_\perp)$ is the inclusive hadron spectrum at transverse momentum p_\perp , and the superscripts refer to the medium and vacuum, respectively. The theoretical calculation of Q invokes two important, mutually competing, mechanisms of the energy loss described below.

The radiative mechanism [21] is caused by deceleration of the colour charge accompanied by the bremsstrahlung of soft gluons; perturbative QCD allows the determination of the soft gluon distribution $I(\omega)$ in terms of a characteristic frequency ω_c .

On the other hand, the collisional mechanism [9]-[17] arises from the elastic encounters with the other partons of the medium; here a QCD motivated drag force permits the evaluation of the average momentum loss Δp_\perp suffered by the test parton over a specified distance L . The collisional loss theory has been recently applied by Mustafa and Thoma [2] (referred to as MT hereafter) assuming a temperature cooling law relevant to chemically equilibrated QGP. The aim of the present paper is to extend their theme to the case where the evolving fugacities have not yet achieved chemical equilibrium.

For the sake of convenience Sec.2 below defines our notations and briefly recapitulates the main formulae derived by MT. The details of our numerical work are presented in Sec.3. Finally, physical interpretations of the results along with some concluding remarks appear in Sec.4.

2 Recapitulation of MT Theory [2]

Step i) In the fireball rest frame a Taylor expansion of the hadron spectrum Σ is made [21]

to rewrite (1) in the standard form

$$\Sigma^{\text{med}}(p_{\perp}) \approx \Sigma^{\text{vac}}(p_{\perp} + \Delta E); \quad \Delta E = \int d\epsilon \epsilon D(\epsilon) \quad (2)$$

where ϵ is the random collisional energy loss over time span t , $E = E_0 + \epsilon$ the random surviving energy, $D(\epsilon)$ the probability distribution that a parton loses the energy ϵ , and ΔE the average energy loss in traversing the distance $L = c t$.

Step ii) Let the instantaneous momentum of the leading parton moving in the transverse x direction be called $\vec{p} = |\vec{p}| \hat{e}_x$. Assuming spatially uniform plasma a Boltzmann transport equation is set-up for the distribution function $D(t, \vec{p})$, Landau's approximation is made in the collision integral, and the resulting Fokker-Planck equation is cast in the form

$$\frac{\partial D}{\partial t} = \frac{\partial}{\partial \vec{p}} [\vec{\mathcal{T}}_1(t, \vec{p}) D] + \frac{\partial^2}{\partial p^2} [\mathcal{T}_2(t, \vec{p}) D]. \quad (3)$$

The transport coefficients $\vec{\mathcal{T}}_1$ and \mathcal{T}_2 are defined in terms of the net instantaneous collision rate $w(t, \vec{p}, \vec{k})$, involving soft momentum transfer \vec{k} , by

$$\vec{\mathcal{T}}_1(t, p) = \int d^3 k w(t, \vec{p}, \vec{k}) \vec{k} \quad (4)$$

$$\mathcal{T}_2(t, \vec{p}) = \frac{1}{2} \int d^3 k w(t, \vec{p}, \vec{k}) k^2 \quad (5)$$

$$w(t, \vec{p}, \vec{k}) = \sum_{j=q, \bar{q}, g} \gamma_j \int \frac{d^3 q}{(2\pi)^3} f_j(t, \vec{q}) v_{\text{rel}} \sigma_j, \quad (6)$$

where j labels different species (quarks, antiquarks, gluons) present in the plasma, γ_j is the degeneracy factor, f_j the species' distribution function depending implicitly on the time through the fugacity $\lambda_j(t)$ and temperature $T(t)$, v_{rel} the relative speed between the test parton and j -th species, and σ_j the associated scattering cross section.

Step iii) Correspondence with classical dissipative motion tells that the function $\vec{\mathcal{T}}_1$ scales like \vec{p} and represents the rate of energy loss $-dE/d\vec{x}$. Hence, a mean drag coefficient $A(t)$ is constructed in one-dimensional notation via

$$\mathcal{A}(t) = \left\langle -\frac{1}{p} \frac{dE}{dL} \right\rangle = \int d^3 p \frac{-\frac{1}{p} \frac{dE}{dL}}{\exp \sqrt{p^2 + m_g^2}/T - 1} / \int d^3 p \frac{1}{\exp \sqrt{p^2 + m_g^2}/T - 1} \quad (7)$$

Since the QGP expected at RHIC and LHC is likely to be out of chemical equilibrium it is necessary to investigate the energy loss in this case [23]. Indeed, even away from chemical equilibrium, dynamical screening remains operational within the HTL-resummed perturbation theory. More explicitly, the collisional energy loss for a heavy quark (mass M)

propagating through a QGP parametrized in terms of the distribution functions $\lambda_q n_F$ and $\lambda_g n_B$, respectively, where $\lambda_{q,g}$ are the fugacity factors describing chemical non-equilibrium, becomes [1]

$$-\frac{dE}{dL} = 2\alpha_s \tilde{m}_g^2 \frac{(1+9/4)}{2} \ln \left[0.920 \frac{\sqrt{ET}}{\tilde{m}_g} 2^{\lambda_q N_f / (12\lambda_g + 2\lambda_q N_f)} \right]. \quad (8)$$

This expression [1, 24] is valid for energetic quarks with $E \gg M^2/T$ and contains for $\lambda_q = \lambda_g = 1$ the original result of [2]. The screening mass parameter is

$$\tilde{m}_g^2 = 4\pi\alpha_s(\lambda_g + \lambda_q N_f/6)T^2/3. \quad (9)$$

The expression reduces to the expression given in Mustafa and Thoma paper by putting $\lambda_g = \lambda_q = 1$. It should be noted that the factor $\frac{(1+9/4)}{2}$ arises due to averaging over the quark and gluon contributions.

Next, the analogy with Einstein's random walk relation is exploited to identify the momentum-averaged diffusion coefficient

$$\mathcal{D}_F(t) = \langle \mathcal{T}_2(t, p) \rangle = \mathcal{A}T^2 \quad (10)$$

so that the evolution equation for the momentum-distribution of the Brownian particle becomes

$$\frac{\partial D}{\partial t} = \mathcal{A} \frac{\partial}{\partial p}(pD) + \mathcal{D}_F \frac{\partial^2 D}{\partial p^2} \quad (11)$$

Step iv) Employing Fourier transform and method of characteristics the above partial differential equation is solved analytically subject to the initial condition $D(p, 0) = \delta(p-p_0)$. The result in terms of length and energy variable is

$$D(L, E) = \frac{1}{\sqrt{\pi\mathcal{W}(L)}} \exp \left[- \frac{(E - E_0 \cdot B(L))^2}{\mathcal{W}(L)} \right], \quad (12)$$

where

$$B(L) = \exp \left(- \int_{\tau_0}^L dt' \mathcal{A}(t') \right), \quad (13)$$

and

$$\mathcal{W}(L) = 4 \int_0^L dt' \mathcal{D}_F(t') \exp \left[2 \int_0^{t'} dt'' \mathcal{A}(t'') \right] B^2(L). \quad (14)$$

Step v) The mean energy $\langle E \rangle$ and average energy loss ΔE are determined from

$$\langle E \rangle = \langle p \rangle \equiv \int_0^\infty dE E D(L, E) = E_0 B(L) \quad (15)$$

and

$$\Delta E = \Delta p \equiv E_0 - \langle E \rangle = E_0 \left(1 - B(L) \right) \quad (16)$$

Eqs.(13, 14) can now be inserted into the basic expression (2) along with the following high-energy parametrization for jet hadronization at RHIC:

$$\Sigma^{\text{vac}}(p_{\perp}) = \text{const} \left(1 + \frac{p_{\perp}}{P_0} \right)^{-\nu}, \quad (17)$$

with $\nu = 8$ and $P_0 = 1.75$ GeV.

Step vi) Finally, the geometry of the head-on heavy ion collision is accounted for by considering a cylindrical plasma of radius R and the test particle moving in the central rapidity region. If the latter was created at the location (r, ϕ) in the transverse plane $z = 0$ then it travels a distance

$$L(r, \phi) = (R^2 - r^2 \sin^2 \phi)^{1/2} - r \cos \phi \quad (18)$$

before leaving the cylinder. Upon averaging (2) over the creation configuration the effective quenching factor becomes

$$Q(p_{\perp}) = \frac{1}{2\pi^2 R^2} \int_0^{2\pi} d\phi \int_0^R d^2r \Sigma^{\text{vac}}(p_{\perp} + \Delta p) / \Sigma^{\text{vac}}(p_{\perp}) \quad (19)$$

which is amenable to direct computations.

3 Numerical Application

Mustafa-Thoma procedure: MT assumed the QGP to expand longitudinally according to Bjorken's boost-invariant hydrodynamics [26] so that the temperature $T(t)$ on the transverse plane decreases according to the scaling law

$$T(t) = T(t_0) \left(\frac{t_0}{t} \right)^{1/3}, \quad (20)$$

where t_0 the instant when the background plasma had just attained local kinetic as well as chemical equilibrium so that all partonic fugacities had become unity. For an $A + B$ collision at RHIC, MT took

$$t_0 = 0.3 \text{ fm}; \quad T_0 = 0.5 \text{ GeV} \quad (21)$$

Table 1: Different sets of initial conditions of the temperature, fugacities and parton number densities at $\tau_0 = 0.7\text{fm}/c$ for RHIC and $\tau_0 = 0.5\text{fm}/c$ for LHC.

	RHIC(1)	LHC(1)	RHIC(2)	LHC(2)	RHIC(3)	LHC(3)
$T(\text{GeV})$	0.55	0.82	0.55	0.82	0.4	0.72
λ_g	0.05	0.124	0.2	0.496	0.53	0.761
λ_q	0.008	0.02	0.032	0.08	0.083	0.118
$n_g(\text{fm}^{-3})$	2.15	18	8.6	72	8.6	72
$n_q(\text{fm}^{-3})$	0.19	1.573	0.76	6.29	0.76	6.29

The momentum averaging in (7) was done using a Boltzmann distribution at temperature $T(t)$ for gluons.

Our Procedure: For the case of longitudinal expansion we know that, in the early stage of evolution, the plasma may achieve equilibrium thermally but not yet chemically. Partonic reactions drive the system towards chemical equilibration through the master rate equations [28]

$$\begin{aligned}
 \frac{\dot{\lambda}_g}{\lambda_g} + 3\frac{\dot{T}}{T} + \frac{1}{\tau} &= R_3(1 - \lambda_g) - 2R_2\left(1 - \frac{\lambda_g^2}{\lambda_q^2}\right), \\
 \frac{\dot{\lambda}_q}{\lambda_q} + 3\frac{\dot{T}}{T} + \frac{1}{\tau} &= R_2\frac{a_1}{b_1}\left(\frac{\lambda_g}{\lambda_q} - \frac{\lambda_q}{\lambda_g}\right), \\
 \left(\lambda_g + \frac{b_2}{a_2}\lambda_q\right)^{3/4} T^3\tau &= \text{const}, \tag{22}
 \end{aligned}$$

where the usual meaning of the symbols can be found in Ref. [28]. Their solutions subject to the initial conditions [29] (Table 1) give the temperature and fugacities at general t , and these enter the distributions $f_j(t, \vec{q})$ of various species written in (6). But the momentum integration in (7) was performed employing an equilibrium Bose-Einstein form at temperature $T(t)$.

Computed Results: Fig.1 plots the collisional drag coefficient A versus elapsed time t for energetic gluons, in the QGP phase of the expanding fireball, obtained from (7). The dashed-dotted line corresponds to MT's equilibrated plasma described by the cooling law (20) whereas other curves refer to our equilibrating plasma governed by the master equations (22). Next, Fig.2 shows the relative energy loss $\Delta p_\perp/p_\perp$ versus the transverse distance L . Finally, Fig.3 displays the effective quenching factor Q versus the transverse momentum p_\perp . Logical explanation of these results is taken-up in the next section.

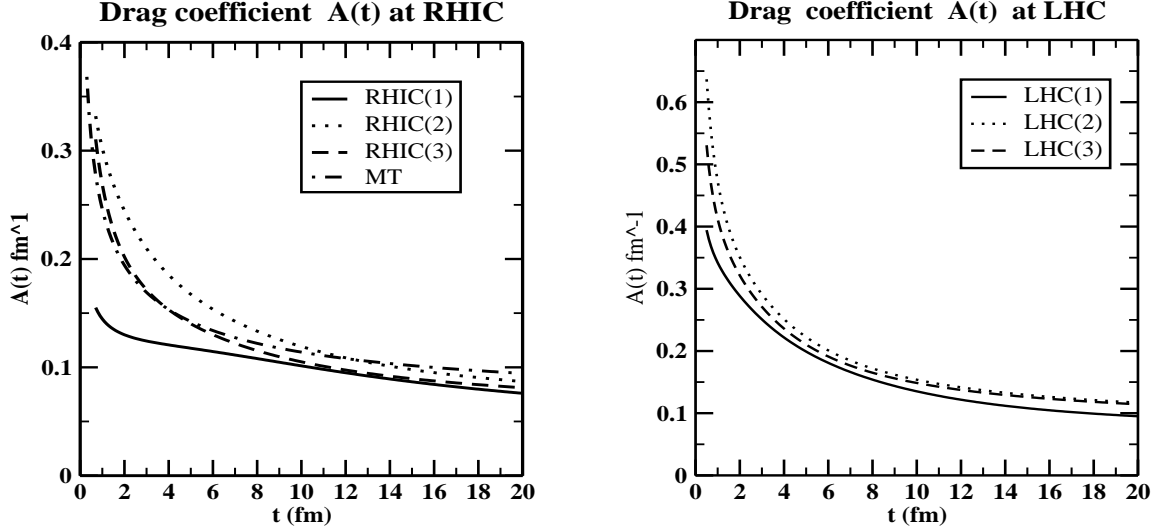


Figure 1: The drag coefficient $\mathcal{A}(t)$ in an expanding QGP. In the left panel, the solid, dotted and dashed line denotes chemically equilibrating QGP corresponding to RHIC(1), RHIC(2) and RHIC(3) initial conditions, respectively. The dashed-dotted line corresponds to MT's equilibrated system. On the other hand right panel corresponds to LHC energy. MT choose the initial values from eq.(21) with $\lambda_q = \lambda_g = 1$ whereas latter takes the initial conditions from Table 1 [29].

4 Interpretations and conclusions

As is well known the distribution function $f_j(t, \vec{q})$ of the j -th species in (6) grows with higher temperature $T(t)$ and fugacity $\lambda_j(t)$. The numerical solution of (20) and (22), with the initial conditions stated, reveals that Mustafa-Thoma fugacities (and hence the transition rates $w(t, \vec{p}, \vec{k})$) are about an order of magnitude more than those in our work at all times of experimental interest. Consequently, in the left panel of Fig.1 the drag coefficient A^{MT} is significantly greater than $A^{\text{RHIC}(1)}$; indeed the ratio $A^{\text{MT}}/A^{\text{RHIC}(1)} \approx 2$ at $t \approx 1 \text{ fm}$. The reason for this difference lies in the fact that MT deals with a fully equilibrated system whereas RHIC(1) deals with the highly unequilibrated system as is evidenced from their initial conditions. As a consequence, gluon density in MT system becomes larger than RHIC(1) resulting higher value of the drag coefficient $A(t)$. At large time (greater than 8 fm), our result does not differ much from MT result because as time elapses chemically unequilibrated system (RHIC(1)) approaches towards chemical equilibrium making the two system alike. However, our calculated value is always less than A^{MT} . Thus equilibrating QGP provides less drag force in comparison to equilibrated QGP.

However for the illustration of the dependence of $A(t)$ on initial parton fugacities,

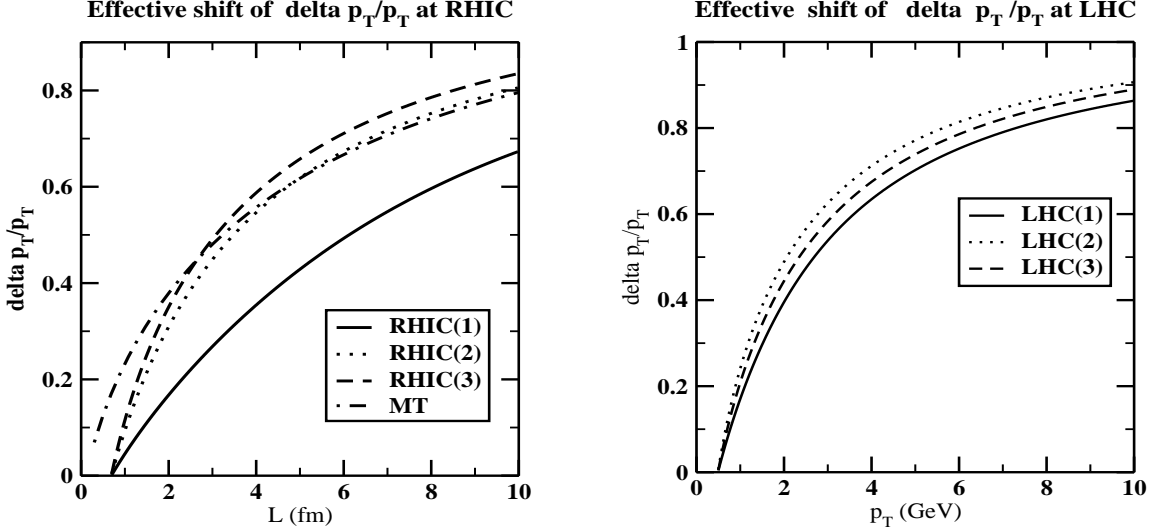


Figure 2: The effective shift of the scaled transverse momentum $\Delta p_{\perp}/p_{\perp}$ as a function of traversed distance L . The notations of the curves are the same as in Fig.1

we have calculated $A(t)$ at RHIC(2) and RHIC(3) [29] where the values of $A(t)$ is not much different from MT. This is due to the fact RHIC(2,3) is not much unequilibrated as RHIC(1) as is evidenced by their initial gluon/quark fugacities or gluon densities compared to RHIC(1).

In the right panel of Fig.1 the drag coefficient $A(t)$ at LHC energy also decreases with time. But our result at LHC energy is always somewhat greater than the value at RHIC. Thus the drag coefficient increases with increase in the center-of-mass energy.

Next, in the left panel of Fig.2 the relative energy loss $\Delta p/p_{\perp} |^{\text{MT}}$ far exceeds $\Delta p/p_{\perp} |^{\text{Our}}$ computed at sizable distances; indeed their mutual ratio is about 1.4 at $L \approx 7$ fm at RHIC(1) energy. This happens because for higher integrand $A(t')$ the function $B(L)$ becomes lower in (13, 16). Of course, in both cases Δp scales almost linearly with p_{\perp} for a given L . In the right panel of the Fig.2 the relative energy loss $\Delta p/p_{\perp} |^{\text{Our}}$ at LHC energy does not differ from the RHIC value. Thus increase in center-of-mass energy in going from RHIC to LHC the relative energy loss in equilibrating QGP will not be affected.

Finally, in the left panel of Fig.3, the quenching factor $Q(p_{\perp})$ is stronger at lower p_{\perp} in our calculation as well as MT calculation and gradually weakens at higher p_{\perp} in agreement with experimental results [20]. However, in our case, the quenching factor $Q(p_{\perp})$ calculated for equilibrating QGP shows less suppression in comparison to quenching factor $Q(p_{\perp})$ calculated for equilibrated QGP. This is again a reflection of the fact that, in contrast to MT equilibrated case, our energy loss Δp_{\perp} is much smaller over the whole assembly of lengths L encountered in (18, 19). Moreover, the qualitative behaviour is same in both the

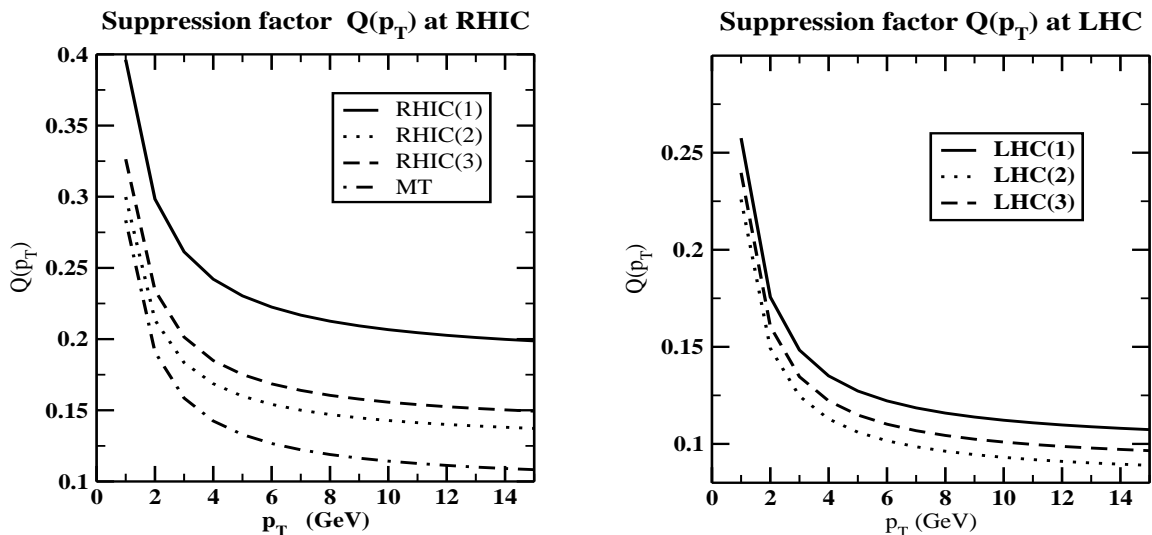


Figure 3: The quenching factor $Q(p_{\perp})$ as a function of transverse momentum p_{\perp} . The notations of the curves are the same as in Fig.1

cases. In right panel of the Fig.3, the quenching factor $Q(p_{\perp})$ shows stronger suppression at LHC energy in comparison to RHIC energy at lower values of the transverse momentum less than $p_{\perp} \approx 8 \text{ GeV}$.

We end the paper with two concluding remarks. Although our assumptions of chemically equilibrating QGP is more realistic than MT's assumption of equilibrated plasma yet the equilibrating QGP will provide weak drag force for the jets in comparison to equilibrated QGP. Thus most jet suppression occurs after the equilibration of the QGP has been achieved. However, this *initial* state effect cannot be neglected. Therefore, jet quenching cannot be exactly called as a *final* state effect.

ACKNOWLEDGEMENTS

BKP is thankful to V.J. Menon for the useful discussion during this work. BKP is also thankful to B. Müller, M. Thoma and M.G.Mustafa for their useful private communication. BKP acknowledges the financial support to IIT Roorkee for the Faculty Initiation Grant and MM thanks to CSIR, New Delhi for his financial support.

References

- [1] R. Baier, D. Schiff, B.G. Zakharovo, Ann. Rev. Nucl. Part. Sci. **50** (2000) 37.
- [2] M. G. Mustafa and Markus Thoma, Acta Phys. Hung. **A 22** (2005) 93.
- [3] M. G. Mustafa, Phys. Rev. **C 72** (2005) 014905.
- [4] M. Gyulassy and M. Plümer, Phys. Lett. B **243** (1990) 432.
- [5] J.D. Bjorken, Fermilab preprint 82/59-THY (1982, unpublished).
- [6] B. Svetitsky, Phys. Rev. D **37** (1988) 2484.
- [7] S. Mrówczyński, Phys. Lett. B **269** (1991) 383.
- [8] Y. Koike and T. Matsui, Phys. Rev. D **45** (1992) 3237.
- [9] E. Braaten and R.D. Pisarski, Nucl. Phys. B **337** (1990) 569.
- [10] E. Braaten and M.H. Thoma, Phys. Rev. D **44** (1991) 1298.
- [11] E. Braaten and M.H. Thoma, Phys. Rev. D **44** (1991) 2625(R).
- [12] H. Vija and M.H. Thoma, Phys. Lett. B **342** (1995) 212.
- [13] P. Romatschke and M. Strickland, *hep-ph/0309093*.
- [14] M.H. Thoma and M. Gyulassy, Nucl. Phys. B **351** (1991) 491.
- [15] M. H. Thoma, Phys. Lett. B **273** (1991) 128.
- [16] M. H. Thoma, J. Phys. G **26** (2000) 1507.
- [17] M. H. Thoma, Eur. Phys. J. C **16** (2000) 513.
- [18] R. Baier, D. Schiff, and B.G. Zakharov, Ann. Rev. Nucl. Part. Sci. **50** (2000) 37.
- [19] E. Wang and X.-N. Wang, Phys. Rev. Lett. **87** (2001) 142301.
- [20] K. Adcox et al. [PHENIX Collaboration], Phys. Rev. Lett. **88** (2002) 022301; C. Adler et al. [STAR Collaboration], Phys. Rev. Lett. **89** (2002) 202301; B.B. Back et al. [PHOBOS Collaboration], *nucl-ex/0302015*.
- [21] R. Baier, Y. L. Dokshitzer, A. H. Mueller, and D. Schiff, JHEP **0109** (2001) 033.
- [22] B. Müller, Phys. Rev. C **67** (2003) 061901(R).

- [23] Mustafa MG, Pal D, Srivastava DK., Phys. Rev. **C57** (1998) 889.
- [24] Baier R, Dirks M, Redlich K., hep-ph/9910353 (1999).
- [25] Braaten E, Thoma MH., Phys. Rev.**D44** (1991) R2625.
- [26] J. D. Bjorken, Phys. Rev. D **27** (1983) 140.
- [27] R. J. Fries, B. Müller and D. K. Srivastava, Phys. Rev. Lett. **90** (2003) 132301.
- [28] T. S. Biro, E. van Doorn, M. H. Thoma, B. Müller, and X.-N. Wang, Phys. Rev. C 48 (1993) 1275.
- [29] X.-N Wang and M. Gyulassy, Phys. Rev. D **44**, 3501 (1991).

Appendix: Jet quenching summarized

The yield of hadron produced with high transverse momentum p_{\perp} in Au+Au collisions at RHIC has recently shown to be significantly suppressed in comparison with the cumulative yield of NN collisions. This effect, so called “Jet quenching” was predicted to occur due to energy loss suffered by hard scattered partons. The energy loss is expected to occur due to interaction of the hard partons with the surrounding dense medium.

There are two contributions to the energy loss of the partons in the medium. One is due to the collisions among the partons in the medium and other due to the radiation emitted by the decelerated colour charge i.e., bremsstrahlung of gluons.

In the initial stage of ultrarelativistic collisions energetic partons are produced from hard collisions energetic partons are produced from hard collisions between the partons of the nuclei. Receiving a large transverse momentum, these partons will propagate through the fireball which might consists of quark-gluon plasma phase for a transitional period of about few fm/c. These high energy partons will manifest themselves as jets leaving the fireball. These energy partons will loose energy due to interaction of the hard partons with the fireball medium. Hence jet quenching will result. The amount of jet quenching might depend on the state of the fireball i.e., QGP or hot hadron gas, respectively. Therefore, jet quenching has been proposed as the possible signature of the QGP formation.

It is difficult to measure the energy loss of the scattered partons directly in heavy-ion collision because of the large multiplicity of the emitted hadrons makes it almost impossible to isolate the resulting jet by the kinematic cut. However, this energy loss of the hard partons may affect the equivalent loss of the energy of the leading hadrons produced it its fragmentation. this is what has been observed at RHIC experiment []. Preliminary data from run 2 at RHIC Au+Au at $\sqrt{s_{NN}} = 200$ GeV confirm the effect observed in run 1 and its interpretation as jet quenching. For pions with $p_{\perp} \approx 5$ GeV/c the measured suppression factor is about 1/5.